IOPscience iopscience.iop.org

Home Search Collections Journals About Contact us My IOPscience

The spatial asymmetric two-dimensional continuous Abelian sandpile model

This article has been downloaded from IOPscience. Please scroll down to see the full text article.

2008 J. Phys. A: Math. Theor. 41 435002

(http://iopscience.iop.org/1751-8121/41/43/435002)

View the table of contents for this issue, or go to the journal homepage for more

Download details:
IP Address: 171.66.16.152
The article was downloaded on 03/06/2010 at 07:17

Please note that terms and conditions apply.

IOP PUBLISHING JOURNAL OF PHYSICS A: MATHEMATICAL AND THEORETICAL

J. Phys. A: Math. Theor. **41** (2008) 435002 (14pp) doi:10.1088/1751-8113/41/43/435002

The spatial asymmetric two-dimensional continuous Abelian sandpile model

N Azimi-Tafreshi, H Dashti-Naserabadi and S Moghimi-Araghi

Department of Physics, Sharif University of Technology, Tehran, PO Box 11155-9161, Iran

E-mail: azimi@physics.sharif.ir and samanimi@sharif.edu

Received 9 June 2008, in final form 10 August 2008
Published 30 September 2008
Online at stacks.iop.org/JPhysA/41/435002

Abstract

We insert some asymmetries into the continuous Abelian sandpile models, such as directedness and ellipticity. We analyze probability distribution of different heights and also find the corresponding field theories. Also we find the fields associated with some height variables.

PACS numbers: 05.65+b, 89.75.Da

(Some figures in this article are in colour only in the electronic version)

1. Introduction

After the seminal work of Bak *et al* [1], sandpile models have been found to be a very helpful framework for the study of self-organized criticality (SOC). SOC is believed to be the underlying reason for the scaling laws seen in a number of natural phenomena [2]. Further investigations showed that the BTW sandpile model has an Abelian property and was renamed an Abelian sandpile model (ASM) [4]. The model is still the simplest, most studied model of SOC, in which many analytical results have been derived. For a good review see [3].

Extensive work has been done on this model, analytical and computational. To name a few, one can list the works by Dhar [4, 5], where the probabilities of some height clusters were computed. In [4], Dhar computed the number of recurrent configurations and showed that all of them occur with equal probability. Later, in [5], Majumdar and Dhar calculated the probabilities of the occurrence of some specific clusters, known as weakly allowed clusters (WAC's). The simplest of these clusters is the one-site cluster of height one. The probabilities of other one-site clusters with height above one were computed in [6]. There are many other analytical results, among them one can mention the results on boundary correlations of height variables and the effect of boundary conditions [7–12], the presence of dissipation in the model [9, 10, 13], field theoretical approaches [9, 14–17], finite size corrections [5, 11] and many other results [3].

 © 2008 IOP Publishing Ltd Printed in the UK

In ASM, the height variable takes only integer values. However there are some other models in which the height variable can take real values. The Zhang model [18] is a continuous energy (height) model with non-Abelian property. When a site topples, the full amount of energy will be transferred in multiples of a finite quasiunit to the nearest neighbors and it is reset to zero. It turns out that the energy variables in the stationary state tend to concentrate around some discrete values of energy. In the thermodynamics limit this model behaves like the ASM and energy tends to be peaked narrowly around the finite set. The other model introduced by Gabrielov called the Abelian avalanche model (AA model) [19], is a deterministic lattice model with continuous time and height values and characterized by the Abelian property. In this paper, it is shown that the distribution of avalanches for a continuous deterministic AA model is identical to the distribution of avalanches for a discrete, stochastic ASM model with the same toppling matrix and driving rate. Ghaffari *et al* [20] introduced a generalized continuous version of the BTW and Zhang model. They have studied the effect of nonconservation in these models for two different types of drives and discussed whether these models exhibit criticality as dissipation is added or not. In the paper by Tsuchiya and Katori [21], the height variables are still integer numbers, but if one takes a large number for the threshold value, it will approach to a continuous model. They have considered the avalanche size distribution and correlation functions when dissipation is present in their model. Also in [22] we considered the model introduced in [20] on a square lattice and studied many of its different properties such as the effect of dissipation on the height probabilities and boundary conditions.

When we let the heights be real numbers, naturally the components of the toppling matrix could be real too. In this paper we consider a continuous ASM and change different components of the toppling matrix. We will do it in a way that adds spatial asymmetries to the model. Two specific asymmetries are considered, one is to introduce a preferred direction. The second is to introduce elliptical asymmetry. The first one is related to a directed sandpile model and the second, as we shall see, results naturally from the original BTW model. We have derived the probability distribution of height variables and also avalanche distributions. Also the field theory associated with these models are considered. The new models are still critical and show scaling relations.

In the following section we first review the continuous ASM. Next we consider the effects of a perturbation that introduces a preferred direction in the model. In section 4, we introduce ellipticity into the model and derive many properties of such a system.

2. The continuous Abelian sandpile model

The continuous Abelian sandpile model (CASM) on a square lattice is defined in [20]. Consider an $L \times L$ square lattice. To each site $u = (i, j)$ a *continuous* height variable, $h(u)$ is assigned, where without loss of generality we assume these variables belong to the interval [0, 4) (in the original paper the interval was taken to be [0,1)). The evolution rules consist of the following:

(1) At each time step, a site is selected randomly and a certain amount of sand is added to it and other height variables are unchanged. The amount of sand added to the site is a random real number in the interval $[p, q] \in [0, 4)$. The distribution function could be any function, but for simplicity we take it to be uniform on the interval $[p, q]$. If height remains below four, the new configuration is stable and we go to the next time step.
(2) If height of the sand at that site becomes equal to or greater than four, the site becomes unstable and topples in the following way: it gives an amount of sand with height one to

either of its neighbors. In other words $h(v) \to h(u) - \Delta^C(u, v)$ for all v, where $\Delta^C(u, v)$ is the toppling matrix of the CASM and is defined as

$$\Delta^C(u, v) \begin{cases} 4 & u = v \\ -1 & |u - v| = 1 \\ 0 & \text{otherwise.} \end{cases} \tag{1}$$

So if the height of a site is $4 + \alpha$, after toppling its height will be α and the heights of neighbors will increase by 1. As a result of this toppling, some of the neighbors may become unstable and an avalanche may occur.

It has been shown in [22] that there is a (many-to-one) mapping from configurations in the CASM to configurations in ASM, which preserves the dynamics, therefore the new model reproduces most of the interesting features of ASM. Also it is shown that the probability distribution is a piecewise constant. The probability of finding a site with height $h \in [k-1, k)$ with $k = 1, 2, 3, 4$ is equal with $p(k)$, the probability of finding a site with height k in the usual ASM. These claims were proved and were found to be in agreement with simulations.

As the heights are continuous, we can take other integer parameters of the model to be real. This has been done for the dissipation parameter in the model [22]. The probability distribution is found when there exists dissipation with different (real) values in [22]. Yet there are some other parameters which are integer in the original model, but may be taken to be real in the new model. In this paper, we consider the amount of sand transferred to the neighbors and let it take different real values and see how the properties of the model are changed.

3. CASM with preferred direction

One of the easiest modifications to the toppling matrix is to introduce a preferred direction; that is, sand grains are more likely to move left rather than right. Such a modification is also studied in the usual ASM [23], but since the toppling matrix components only take integer values, the only possibility is to send two sand grains to the left and nothing to the right. The same can be done in the vertical direction. If this is the case, then the toppling matrix will be upper triangular and all the configurations will be recurrent [23]. However, in our model we are able to control the amount of directedness: when a site is toppled, then $1 + \epsilon$ grains of sand move left and $1 - \epsilon$ grains of sand move right. Clearly $\epsilon = 0$ corresponds to the usual ASM and $\epsilon = 1$ corresponds to the case mentioned above, provided we add both horizontal and vertical directedness.

Several properties of the model can be studied, the probability distribution, the corresponding action, the avalanche distributions, etc. The probability distribution of finding different heights is sketched in figure 1 for some different values of ϵ when for both x and y directions the toppling rule is directed. As we see, still we have the same step-like pattern as in the case of the undirected CASM. Some new small steps have appeared the lenghts of which are proportional to ϵ. As ϵ becomes larger, these steps become longer and gradually the original pattern fades away. At $\epsilon = 1$ corresponding to the full directed model, the probability distribution becomes uniform as is shown in [23] that each of the stable configurations occurs with equal probability.

The avalanche distribution is also studied in this model. System sizes from 64 to 1024 have been investigated. Starting with a lattice of randomly distributed heights $h \in [1, 4)$, the system evolves to reach steady state. After that, we begin the measurements. The measurements are averaged over about 10^7 avalanches. One of the characteristics of an avalanche is the avalanche size s that is the total number of toppling events in it. In the critical steady state

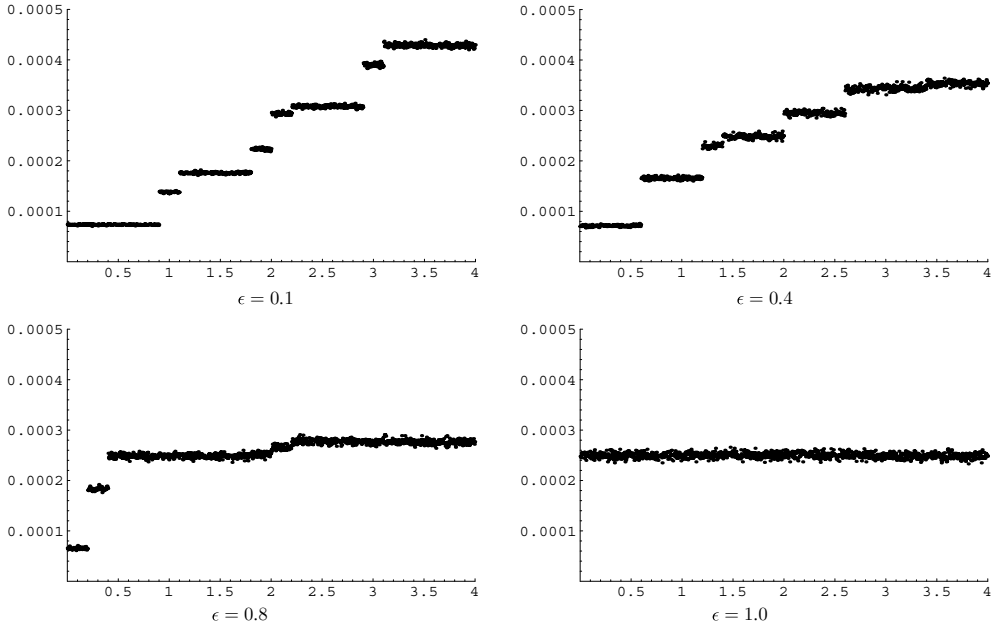

Figure 1. The probability density profile of height variables.

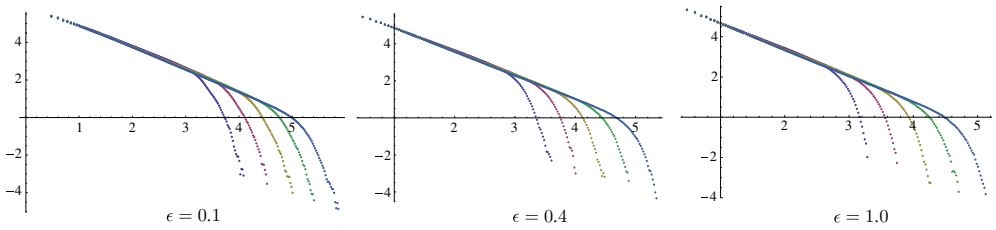

Figure 2. Avalanche size distribution for $\epsilon = 0.1, 0.4, 1.0$ and for lattice sizes $L = 64, 128, 256, 512, 1024$.

the corresponding probability distribution should obey power-law behavior characterized by exponent τ_s:

$$P(s) \propto s^{-\tau_s}. \tag{2}$$

Figure 2 displays the obtained results for the distribution $P(s)$ of different system sizes for three different values of $\epsilon = 0.1, 0.4, 1.0$ when for both x and y directions the toppling rule is directed. A power-law fit to the straight portion of these curves yields the exponents $\tau_s(L)$. Figure 3 shows a plot of the exponents $\tau_s(L)$ versus $1/\log L$ for $\epsilon = 0, 0.1, 0.4$ and 1. This allows us to extract the exponent $\tau_s(\infty)$. For the cases shown in figure 3, this turns out to be 1.26 ± 0.06 for $\epsilon = 0$, 1.31 ± 0.08 for $\epsilon = 0.1$, 1.38 ± 0.08 for $\epsilon = 0.4$ and $\tau_s = 1.38 \pm 0.08$ for $\epsilon = 1$. It is worth mentioning that due to the finite size of the lattice the magnitude of the slope is smaller for small values of s. Yet it can be seen that the system is critical and self-organized. There is no characteristic length in the model and finite-size scaling is clearly observed in figure 2. One can compare the results obtained for the case of $\epsilon = 1$ with the exact

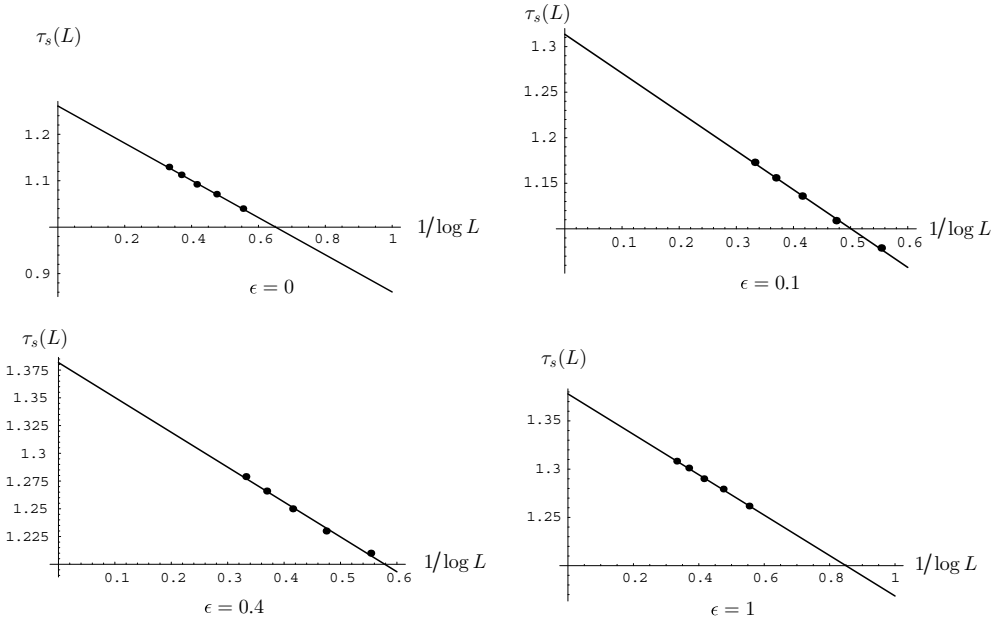

Figure 3. The exponent $\tau_s(L)$ is a linear function of $1/\log L$. The intersection with the vertical axis gives $\tau_s(\infty)$.

result [23]. In [23], the critical exponents are exactly determined for a fully directed model in arbitrary dimension d. In $d = 2$, τ_s equal to $4/3$ in agreement with the result obtained here.

It is seen from the above results that the exponent τ_s seems to increase as ϵ becomes larger which is expected due to the known behavior of directed sandpile models. The value of τ_s for $\epsilon = 0.4$ is equal to the same value for $\epsilon = 1.0$. This is possibly because adding directness is a relevant perturbation and the large-scale behavior of the system is the same as the fully directed model. In this case, the SOC is preserved but in a different universality class.

In the continuum limit, we can assign an action to the theory. As in the steady state, only recurrent configurations appear, and they appear with equal probability, the partition function is simply equal to the total number of recurrent configurations, that is, the determinant of the toppling matrix. Such determinants could be written in terms of an integral over Grassmann variables:

$$\det \Delta = \int \mathrm{d}\theta_i \, \mathrm{d}\bar{\theta}_i \exp(\theta_i \Delta_{ij} \bar{\theta}_j). \tag{3}$$

In this way we can obtain the action of the theory. If lattice spacing is small, one can go to the continuum limit and find a field theoretic action for the theory. In the case of usual ASM the action turns out to be the $c = -2$ logarithmic conformal theory action [14, 24]:

$$S_{c=-2} \propto \int \bar{\partial}\theta \, \partial\bar{\theta}. \tag{4}$$

For the theory defined above, the action is more or less the same, but there are some added terms due to directedness:

$$S_{\mathrm{dir}} \propto \int (\bar{\partial}\theta \, \partial\bar{\theta} + \theta(a\partial + \bar{a}\bar{\partial})\bar{\theta}), \tag{5}$$

where a is a constant proportional to ϵ with dimension of length. This new term grows under a renormalization group, therefore the large-scale properties of the model is given by the fully directed model.

4. Elliptical asymmetry

In the previous section, we assumed that the lattice has a preferred direction. The field associated with this deformation was a relevant one and hence we expected that the theory shows different characteristics on large scales. Also the toppling matrix was not symmetric: the amount of sand transferred from sites i to j is not necessarily equal to the amount of sand transferred from j to i. Therefore one cannot apply the burning test to the model. However it is possible to modify the toppling matrix in a way that it remains symmetric and, as we shall see, the added term to the action would not be relevant.

We assume that the vertical links can carry an amount of sand equal to $1 - \epsilon$ and the horizontal links can carry an amount of sand equal to $1 + \epsilon$ ($0 \leqslant \epsilon \leqslant 1$). In this way the total amount of sand removed from a toppled site is 4 and the mass of sand is conserved. The new toppling matrix is symmetric, but in real space, the x-direction is quite different from the y-direction; in fact, we have added some ellipticity to the system and therefore it does not have full rotational symmetry, however this deformation preserves scale symmetry.

If we go back to the original BTW paper [1], we observe that elliptical asymmetry could arise naturally in their model. In their paper, BTW first define a one-dimensional model and using a specific transformation, express it in some other parameters. We can do the same thing to a two-dimensional model to arrive at the BTW model, however it can easily be seen that if we apply the same transformation to the two-dimensional model, we will not arrive at the BTW model, instead we arrive at a model with elliptical asymmetry. Let us explain this in more detail. In the one-dimensional model, an ordered array of heights z_i is involved. Sand grains enter from left and leave from right. If the difference of the heights of two neighbors becomes more than two a sand grain moves to right. The slope parameters h_i are defined as $h_i = z_i - z_{i+1}$. Then as a result of 'toppling' at site i we will have $h_i \to h_i - 2$ and $h_{i\pm1} \to h_{i\pm1} + 1$. The generalization to two dimensions would be to define the slope parameters as $h_i = 2z_i - z_{i,R} - z_{i,D}$, where $z_{i,R}$ and $z_{i,D}$ are the height variables of the sites to the right of site i and below it, respectively. As for the dynamics if the slope parameter of a site (mean value of the slope there) is more than a threshold value, one sand grain moves right and one sand grain moves downward. The dynamics in terms of the h variables would be $h_i \to h_i - 4$, $h_{i,L;R;D;U} \to h_{i,L;R;D;U} + 2$ and $h_{i,RU;LD} \to h_{i,RU;LD} - 1$, where $h_{i,RU;LD}$ are the slope parameters of right-up and left-down next nearest neighbors of site i. As we see there is an asymmetry in the two diagonal directions and the system does not have full rotational symmetry.

The probability distribution of finding different heights is sketched for $\epsilon \in \{0.1, 0.4, 1.0\}$ in figure 4. The simulation is done on a 1024×1024 lattice averaging over 10^7 samples. We still have major and minor steps when ϵ is small. As ϵ becomes greater, the minor steps become larger and at $\epsilon = 1$ we have a two-step graph, which indicates that the model is now effectively one dimensional.

The avalanche distribution is also studied in this model. Just as for the case of the directed CASM, system sizes from 64 to 1024 have been investigated. Again, starting with a lattice of randomly distributed heights $h \in [1, 4]$, the system evolves to reach steady state. After that, the measurements begin. The measurements are averaged over about 10^7 avalanches. Probability distribution of avalanche size is sketched for $\epsilon = 0.1, 0.4$ in figure 5. The case of $\epsilon = 1.0$ is totally different, as corresponds to one-dimensional ASM.

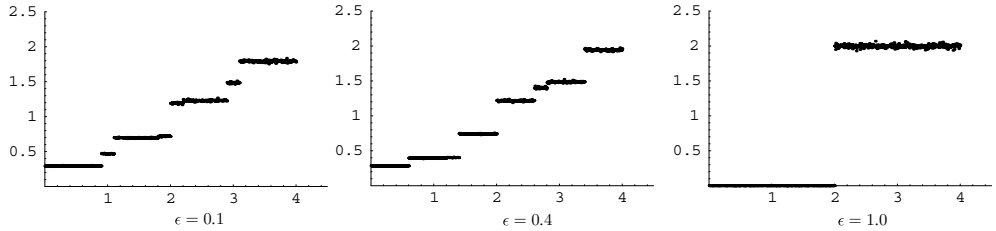

Figure 4. The probability density profile of height variables in the presence of elliptical asymmetry.

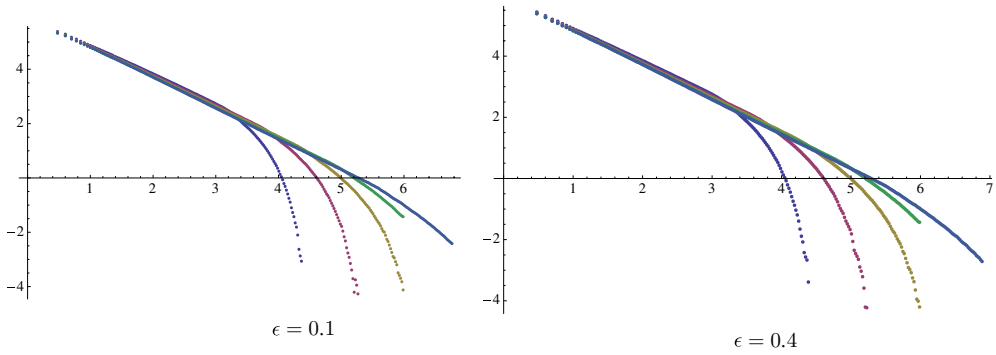

Figure 5. The avalanche size distribution in a system with elliptical asymmetry.

Using the same tools, the slope $\tau_s(\infty)$ for different values of ϵ can be obtained, for example we have $\tau_s(\infty)_{\epsilon=0.1} = 1.25 \pm 0.06$ and $\tau_s(\infty)_{\epsilon=0.4} = 1.24 \pm 0.06$. Again the system shows finite-size scaling and is critical, but there are no remarkable variations in exponents such as τ_s as ϵ is varied. It is possible that the exponents belong to the same universality class.

4.1. One-site height probability

In the CASM with no asymmetries, one is able to find the probability of having any height in the interval [0, 1]. This is done using the burning algorithm [5]: consider the recurrent configurations with the property that the height of site i belongs to [0, 1]. As this site burns after all of its neighbors, it should be a leaf in the corresponding spanning tree. Therefore, the total number of such configurations could be obtained by counting the number of spanning trees in which site i is a leaf. In the modified model the same arguments hold for $h \in [0, 1-\epsilon)$, because the burning test still works and any site with $h \in [0, 1-\epsilon)$ has to be a leaf in the corresponding spanning tree. Note that as we have links with weight $1+\epsilon$, the sites with $h \in [1-\epsilon, 1+\epsilon]$ may not be a leaf.

Similar to the way we find the probability of height one in ASM, we modify the weights of the toppling matrix to ensure that site i is a leaf. This modification of weights is only done on a finite number of lattice bonds, therefore the probabilities corresponding to these local restrictions can be calculated in terms of a finite-dimensional determinant.

We modify the original model by removing the bonds to three neighbors of site i such that only one bond connects site i to the system. All four possible choices to cut the bonds are not equivalent, there are two different modifications: A_1 and A_2 shown in figure 6. In the case A_1,

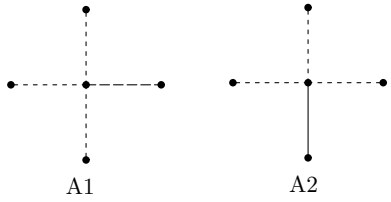

Figure 6. Two types of bond modification.

we delete all neighbor bonds of site i except for a left or a right one which has weight $1+\epsilon$, and change the weight of this remaining bond to $1-\epsilon$ to ensure the height of site i would not be more than $1-\epsilon$. In the case A_2, one of the vertical bonds with the weight $1-\epsilon$ remains unchanged and connects site i to the system.

The two new toppling matrices are of the form $\Delta^{(1)} = \Delta - B^{(1)}$ and $\Delta^{(2)} = \Delta - B^{(2)}$ respectively where $B^{(1)}$ and $B^{(2)}$ are defect matrices:

$$B^{(1)} = \begin{pmatrix} 3+\epsilon & -1+\epsilon & -1-\epsilon & -1+\epsilon & -2\epsilon \\ -1+\epsilon & 1-\epsilon & 0 & 0 & 0 \\ -1-\epsilon & 0 & 1+\epsilon & 0 & 0 \\ -1+\epsilon & 0 & 0 & 1-\epsilon & 0 \\ -2\epsilon & 0 & 0 & 0 & 2\epsilon \end{pmatrix}, \tag{6}$$

$$B^{(2)} = \begin{pmatrix} 3+\epsilon & -1-\epsilon & -1+\epsilon & -1-\epsilon \\ -1-\epsilon & 1+\epsilon & 0 & 0 \\ -1+\epsilon & 0 & 1-\epsilon & 0 \\ -1-\epsilon & 0 & 0 & 1+\epsilon \end{pmatrix}. \tag{7}$$

As we have left-right and up-down symmetries, the number of configurations where $h_i \in [0, 1-\epsilon)$ is proportional to $N = 2(\det \Delta^{(1)} + \det \Delta^{(2)})$. So the probability of finding at most $1-\epsilon$ sand grains at a site is given by

$$P(1-\epsilon) = \frac{N}{4 \det \Delta} = \frac{1}{2} \det(I - B^{(1)}G) + \det(I - B^{(2)}G), \tag{8}$$

where $G = \Delta^{-1}$, is the Green function matrix with the following integral form:

$$G_{ij} - G_{00} = \int_{-\pi}^{\pi} \frac{\mathrm{d}p_i}{2\pi} \int_{-\pi}^{\pi} \frac{\mathrm{d}p_j}{2\pi} \frac{\cos(ip_i)\cos(jp_j) - 1}{4 - 2(1+\epsilon)\cos p_i - 2(1-\epsilon)\cos p_j}. \tag{9}$$

The new toppling rules with elliptic asymmetry in the CASM make the values of the Green function dependent on the orientation of two sites in addition to their distances. Hence their calculation is a bit trickier. For example, in the symmetric case it is enough to calculate G_{ii} and all other components of G can be obtained easily thereafter. We have computed the Green functions analytically and a few of them which were necessary to derive $P(1-\epsilon)$ are listed in the appendix. Using these Green functions, the determinants can be computed and $P(1-\epsilon)$ evaluated. The formula is a very long expression and we do not present it here, we have sketched it in figure 7. The result is in very good agreement with the simulations. As we see, for $\epsilon = 0$ we arrive at the well-known result $P(1)$ in BTW model. The probability gradually decreases until it vanishes at $\epsilon = 1$ which is to be expected. It is also possible to evaluate other one-site probabilities such as the probability $h \in [1-\epsilon, 1+\epsilon)$. In these cases, you have some non-local constraints, such as higher than one one-site probabilities in standard ASM.

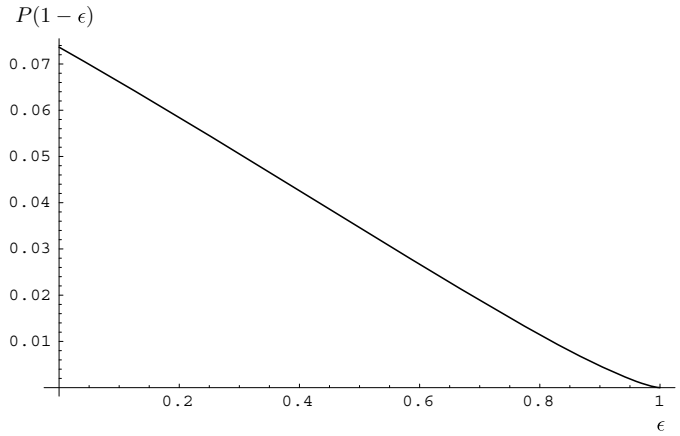

Figure 7. The probability $P(1-\epsilon)$ as a function of ϵ.

4.2. Two-point correlation function

Again, using the same scheme introduced by [5], one is able to find the correlation functions for finding sites with height less than $1-\epsilon$. Making the modifications according to configurations A_1 and A_2 in the vicinity of any two sites, it is possible to find the probability that both sites have heights less than $1-\epsilon$. In order to compute this joint probability, we consider one site at the origin and another at $i = (r, \theta)$. There are four different cases depending on how we modify the toppling rules: the defect matrices associated with either site could be $B^{(1)}$ or $B^{(2)}$. Collecting all the four possible configurations, one finds:

$$P(1-\epsilon, 1-\epsilon) = \frac{1}{4}\left(\sum_{n,\acute{n}=1}^{2} \det\left(I - \begin{pmatrix} G_{00} & G_{0i} \\ G_{i0} & G_{ii} \end{pmatrix}\begin{pmatrix} B^{(n)} & 0 \\ 0 & B^{(\acute{n})} \end{pmatrix}\right)\right). \quad (10)$$

The G blocks denote Green function matrices for the two sites and $G_{0i} = (G_{i0})^t$. The short-distance Green functions are given in the appendix, therefore to evaluate the above determinants at the scaling limit we have to know the expansion of the Green function at large distances. This can be obtained by solving the deformed continuum Laplace equation:

$$G(r,\theta) = \frac{1}{\sqrt{1-\epsilon^2}}\left(-\frac{1}{2\pi}\ln r - \frac{1}{4\pi}\ln\left(\frac{\cos^2\theta}{1+\epsilon} + \frac{\sin^2\theta}{1-\epsilon}\right) - \frac{\gamma}{2\pi} - \frac{\ln 8}{4\pi} + \frac{1}{24\pi r^2\left(\frac{\cos^2\theta}{1+\epsilon} + \frac{\sin^2\theta}{1-\epsilon}\right)} + \cdots\right), \quad (11)$$

where $\gamma = 0.577\ldots$ is the Euler–Mascheroni constant. Using all these, we are ready to find the two-point probability:

$$P(h_0 < 1-\epsilon, h_r < 1-\epsilon) = (P(1-\epsilon))^2 + \frac{f(\epsilon,\theta)}{r^4} + \cdots, \quad (12)$$

where f is derived as an analytic function in terms of ϵ and θ. Again it is a very long expression which we do not present here. We have sketched the function f in the polar coordinate for two different values of $\epsilon = 0.1$ and 0.2 in figure 8. The result shows that the correlations are long ranged and have scaling property though there is no rotational symmetry. Also the amount of this anisotropy depends on ϵ.

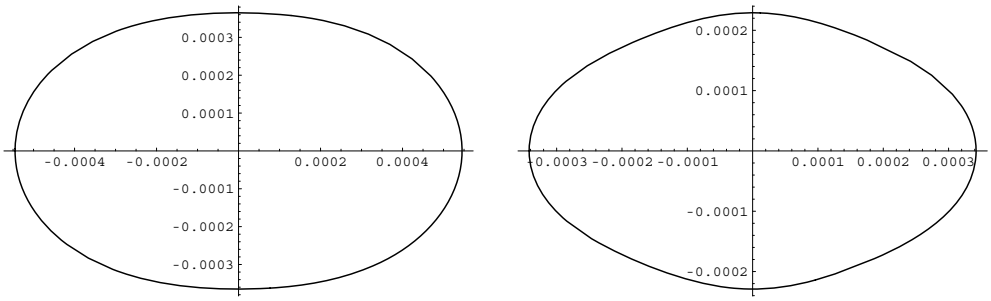

$\epsilon = 0.1$ $\epsilon = 0.2$

Figure 8. The degree of rotational asymmetry of two-point functions for $\epsilon = 0.1$ and 0.2.

4.3. Boundary effects on height $1 - \epsilon$ *probability*

As boundary sites play an important role in sandpile models, it would be interesting to consider the model in the presence of different boundary conditions (BCs). We consider two types of boundary conditions, open and closed [25], according to the toppling rules in our model. In the case of open BC, we set $\Delta_{ii} = 4$ for the boundary sites. This means that the amount of sand leaving the system when a boundary site topples is $1 - \epsilon$ or $1 + \epsilon$ depending on whether the site is on a horizontal or vertical edge. For closed BC we set $\Delta_{ii} = 3 + \epsilon$ on the horizontal edge and $\Delta_{ii} = 3 - \epsilon$ for the vertical edge so that there will be no dissipation on the boundary. It maybe hard to keep track of vertical and horizontal edges, an easier way is to consider $\epsilon \in (-1, 1)$, so the transformation $\epsilon \to -\epsilon$ would interchange vertical and horizontal edges.

For simplicity, we assume that the model is defined on the upper half-plane and the open/closed boundary is located at $y = 1$. Let us compute the probability of having an amount of sand less than $1 - \epsilon$ at site $i = (0, y)$ in the upper half-plane. To this end we have to compute the open and closed Green functions for two sites $i_1 = (x_1, y_1)$ and $i_2 = (x_2, y_2)$. This could be done using the image method:

$$G^{\mathrm{op}}(x_1, y_1; x_2, y_2) = G(x_1 - x_2, y_1 - y_2) - G(x_1 - x_2, y_1 + y_2), \tag{13}$$

$$G^{\mathrm{cl}}(x_1, y_1; x_2, y_2) = G(x_1 - x_2, y_1 - y_2) + G(x_1 - x_2, y_1 + y_2 - 1). \tag{14}$$

The calculations of height $1 - \epsilon$ probability in the presence of the boundary are similar to that on the plane. There are three different configurations as shown in figure 9, therefore[1]

$$P^{\mathrm{op,cl}}(1 - \epsilon, y) = \tfrac{1}{4}\left(2 \det\left(I - B^{(1)} G^{\mathrm{op,cl}}_{h,A}\right) + \det\left(I - B^{(2)} G^{\mathrm{op,cl}}_{h,B}\right) + \det\left(I - B^{(2)} G^{\mathrm{op,cl}}_{h,C}\right)\right). \tag{15}$$

Using equation (11) we are able to calculate the determinants for large distances from the boundary, then we find that the probability for height $1 - \epsilon$ at a distance y from the boundary is

$$P^{\mathrm{op,cl}}(1 - \epsilon, y) = P(1 - \epsilon) \pm \frac{S(\epsilon)}{y^2} + O\left(\frac{1}{y^4}\right), \tag{16}$$

where the constant term $P(1 - \epsilon)$ is the bulk probability for a site to have a height of at most $1 - \epsilon$ and is given by equation (8). The leading term that depends on the distance from

[1] It turns out that the configurations B and C have the same contribution at large distances.

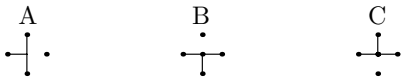

Figure 9. Three different configurations to modify the toppling matrix near a boundary.

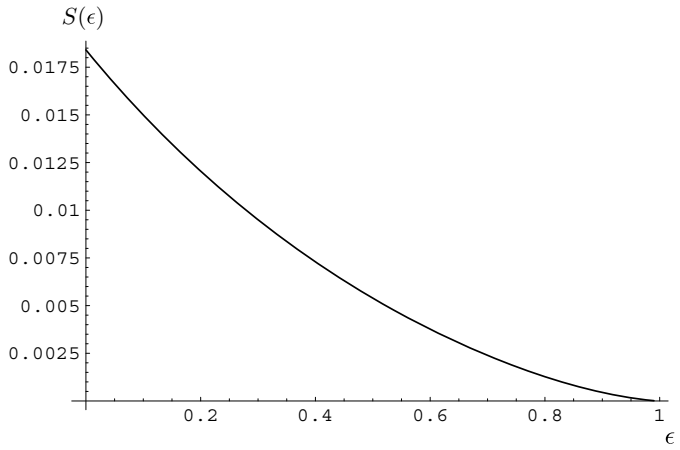

Figure 10. $S(\epsilon)$ as a function of ϵ.

boundary falls off as $1/y^2$ with coefficient $S(\epsilon)$ which is a complicated analytic function of ϵ and is sketched in figure 10. The plus sign corresponds to the open boundary condition and the minus sign to closed ones. It can be shown that this probability at a distance x from a vertical open or closed boundary has a similar behavior.

4.4. Field theoretic description

As mentioned before, the number of different recurrent configurations of the sandpile model (the partition function) is given by determinant of the toppling matrix Δ which leads to the action of $c = -2$ logarithmic conformal field theory (equation (4)). We rewrite the action in x–y coordinates:

$$S = \int -\theta\partial_x^2\bar{\theta} - \theta\partial_y^2\bar{\theta}. \tag{17}$$

The lattice rotational symmetry is broken when we apply elliptic asymmetry in the toppling rules. So it is expected that the field theory describing our model not to be conformal invariant. The perturbed action turns out to be

$$S \sim \int -\theta\partial_x^2\bar{\theta} - \theta\partial_y^2\bar{\theta} - \epsilon\left(\theta\partial_x^2\bar{\theta} - \theta\partial_y^2\bar{\theta}\right), \tag{18}$$

which is rotationally asymmetric.

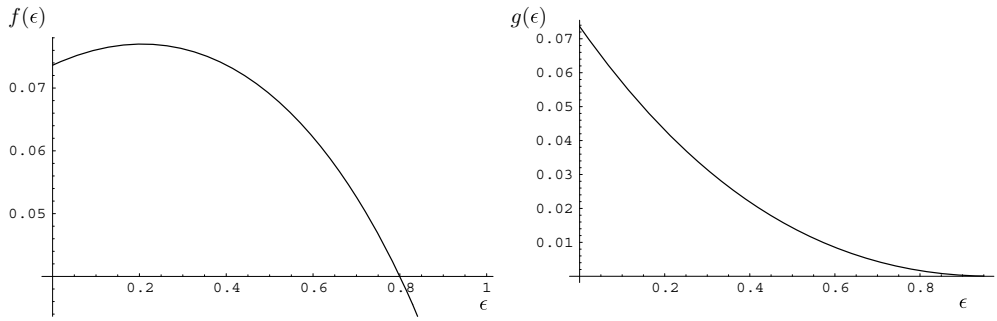

Figure 11. $f(\epsilon)$ and $g(\epsilon)$ are sketched as functions of ϵ.

In this field theory, following the Grassmaniann method used in [14], it is possible to assign a scaling field to the height variable belonging to the $[0, 1-\epsilon)$ interval. The probability of height $1-\epsilon$ can be written as

$$P(1-\epsilon) = \frac{\int \mathrm{d}\theta_i \int \mathrm{d}\bar{\theta}_j \exp\left(\sum \theta_i \Delta_{ij} \bar{\theta}_j\right) \frac{1}{2}\left(\exp\left(-\theta_i B_{ij}^{(1)} \bar{\theta}_j\right) + \exp\left(-\theta_i B_{ij}^{(2)} \bar{\theta}_j\right)\right)}{\int \partial\theta_i \int \mathrm{d}\bar{\theta}_j \exp\left(\sum \theta_i \Delta_{ij} \bar{\theta}_j\right)}, \tag{19}$$

which resembles the expectation value of the field $(1/2)(\exp(-\theta B^{(1)}\bar{\theta}) + \exp(-\theta B^{(2)}\bar{\theta}))$. Following [14], we can assign a field to this height variable in the following way:

$$\phi(1-\epsilon) = \tfrac{1}{2}\left\langle\!\left\langle \exp\left(-\theta_i B_{ij}^{(1)} \bar{\theta}_j\right) + \exp\left(-\theta_i B_{ij}^{(2)} \bar{\theta}_j\right)\right\rangle\!\right\rangle, \tag{20}$$

where $\langle\langle \cdots \rangle\rangle$ means that we have to contract all θ's and $\bar{\theta}$'s except two. In the contraction we have to use the Green functions given in the appendix. Doing all this and going to the continuum limit we will arrive at

$$\phi(1-\epsilon) = -(f(\epsilon)\partial_x\theta\partial_x\bar{\theta} + g(\epsilon)\partial_y\theta\partial_y\bar{\theta}), \tag{21}$$

where $f(\epsilon)$ and $g(\epsilon)$ are complicated functions with long-range behavior that are plotted in figure 11.

As we see, setting $\epsilon = 0$ we will arrive at the known ASM field. As we increase ϵ the function g gradually approaches zero and is always positive. However the function f increases for values up to $\epsilon \simeq 0.2$ and then decreases and becomes zero at $\epsilon = 1$. This is natural, because the limit $\epsilon \to 1$ means you want to find the field associated with the probability of height h be in the interval $[0, 1-\epsilon] = \emptyset$, therefore the field should be zero.

At any case it is very interesting to investigate this new field theory. In this theory, the scale symmetry is preserved and we expect criticality. However rotational symmetry is broken and we do not have the full conformal invariance, though the system is still solvable from field theoretic point of view. Possibly one can investigate this model in the context of perturbed conformal field theory [26, 27]. It can be argued that the action (18) could become symmetric if you rescale horizontal and vertical directions with suitable (and different) scale parameters [28], therefore this new theory should be identical with the previous one. This argument, if applied to the action is completely correct, and if one constructs the field theory through defining the correlation functions the two theory will be identical. But if we ask questions about the field assigned to physical properties, such as the probability of height of a site being less than $1-\epsilon$, the situation becomes more complicated and it is not easy to find a way to relate the corresponding fields in the two theories. For example the field associated with the probability of height of a site being less than $1-\epsilon$ in the ordinary CASM is $(1-\epsilon)\phi_1$, where ϕ_1 is the field of the height one in ASM. However the same field in an asymmetric case is

given by equation (21) and could not be derived from ϕ_1 via a simple rescaling. On the other hand it has been seen that the scaling exponent τ_s is not sensitive to the value of ϵ. Putting all these together, it seems that the elliptical asymmetry do not change the universality class of the theory.

It is also possible to restore the rotational symmetry statistically. If we assume the on-site asymmetries have quenched randomness; that is, on some sites ϵ takes positive values and on some others it takes negative values, then there is no preferred direction statistically. The model should be formulated with more care, however it is very interesting to see whether adding such quenched randomness will take the system to a new fixed point. Work in this direction is in progress.

Acknowledgment

We would like to thank D Dhar for his helpful comments and careful reading of the manuscript.

Appendix

We have collected some values of the Green function G that we have used throughout the paper:

$$G(1,1) = -\frac{1}{\pi\sqrt{1-\epsilon^2}},$$

$$G(0,1) = \frac{\arcsin\left(\sqrt{\frac{1-\epsilon}{2}}\right)}{\pi(\epsilon-1)},$$

$$G(1,0) = -\frac{\left(\pi - 2\mathrm{arccotan}\left(\frac{1+\epsilon}{\sqrt{1-\epsilon^2}}\right)\right)}{2\pi(1+\epsilon)},$$

$$G(0,2) = -\frac{2(1+\epsilon)}{\pi(-1+\epsilon)\sqrt{1-\epsilon^2}} - \frac{4\arcsin\left(\sqrt{\frac{1-\epsilon}{2}}\right)}{\pi(-1+\epsilon)^2},$$

$$G(2,0) = \frac{2\left(\sqrt{1-\epsilon^2} - \pi + 2\mathrm{arccotan}\left(\sqrt{\frac{1+\epsilon}{1-\epsilon}}\right)\right)}{\pi\,(1+\epsilon)^2}.$$

References

[1] Bak P, Tang C and Wiesenfeld K 1987 *Phys. Rev. Lett.* **59** 381
[2] Jensen H J 1998 *Self-Organized Criticality* (Cambridge: Cambridge University Press)
[3] Dhar D 1999 arXiv:cond-mat/9909009
[4] Dhar D 1990 *Phys. Rev. Lett.* **64** 1613
Dhar D 1990 *Phys. Rev. Lett.* **64** 2837
[5] Majumdar S N and Dhar D 1992 *Physica* A **185** 129
[6] Priezzhev V B 1994 *J. Stat. Phys.* **74** 955
[7] Ivashkevich E V 1994 *J. Phys. A: Math. Gen.* **27** 3643
[8] Jeng M 2005 *Phys. Rev.* E **71** 016140 (arXiv:cond-mat/0407115)
[9] Jeng M 2005 *Phys. Rev.* E **71** 036153 (arXiv:cond-mat/0405594)
[10] Jeng M 2004 *Phys. Rev.* E **69** 051302 (arXiv:cond-mat/0312656)
[11] Ruelle P 2002 *Phys. Lett.* B **539** 172 (arXiv:hep-th/0203105)
[12] Ruelle P 2007 *J. Stat. Mech.* P09013 (arXiv:0707.3766)
[13] Piroux G and Ruelle P 2004 *J. Stat. Mech.* P10005 (arXiv:hep-th/0407143)
[14] Moghimi-Araghi S, Rajabpur M A and Rouhani S 2005 *Nucl. Phys.* B **718** 362 (arXiv:cond-mat/0410434)

[15] Jeng M, Piroux G and Ruelle P 2006 *J. Stat. Mech.* **0610** P10015 (arXiv:cond-mat/0609284)
[16] Mahieu S and Ruelle P *Phys. Rev.* E **64** 066130 (arXiv:hep-th/0107150)
[17] Moghimi-Araghi S and Nejati A 2007 *J. Phys. A: Math. Theor.* **40** 11277 (arXiv:cond-mat/0612224)
[18] Zhang Y 1989 *Phys. Rev. Lett.* **63** 470
[19] Gabrielov A 1993 *Physica* A **195** 253
[20] Ghaffari P, Lise S and Jensen H J 1997 *Phys. Rev.* E **56** 6702
[21] Tsuchiya T and Katori M 2000 *Phys. Rev.* E **61** 1183
[22] Azimi-Tafreshi N, Lotfi E and Moghimi-Araghi S 2007 arXiv:0710.3292
[23] Dhar D and Ramaswamy R 1989 *Phys. Rev. Lett.* **63** 1659
[24] Ivashkevich E V and Priezzhev V B 1998 *Physica* A **254** 97–116
[25] Brankov J G, Ivashkevich E V and Priezzhev V B 1993 *J. Physique* I **3** 1729–40
[26] Zamolodchikov A B 1989 *Adv. Stud. Pure Math.* **19** 641
[27] Rajabpour M A and Rouhani S 2006 *Nucl. Phys.* B **754** 283–92
[28] Dhar D 2008 Private communication